American Journal of Nano Research and Applications
2017; 5(5): 61-68
http://www.sciencepublishinggroup.com/j/nano
doi: 10.11648/j.nano.20170505.11
ISSN: 2575-3754 (Print); ISSN: 2575-3738 (Online)

Photocatalytic Degradation of Citric Acid in Wastewater in Presence of Visible Light by La:Ni:TiO_2 Nanocomposite

Azad Kumar*, Gajanan Pandey

Department of Applied Chemistry, School for Physical Sciences Babasaheb Bhimrao Ambedkar University, Lucknow, India

Email address:
kumarazad20@gmail.com (A. Kumar)
*Corresponding author

To cite this article:
Azad Kumar, Gajanan Pandey. Photocatalytic Degradation of Citric Acid in Wastewater in Presence of Visible Light by La:Ni:TiO_2 Nanocomposite. *American Journal of Nano Research and Applications*. Vol. 5, No. 5, 2017, pp. 61-68. doi: 10.11648/j.nano.20170505.11

Received: July 4, 2017; **Accepted**: July 13, 2017; **Published**: September 16, 2017

Abstract: In this study, nanocomposites of La:Ni:TiO_2 nanocomposite was prepared by the co-precipitation method. The material was found in the nano dimension by the SEM and TEM analysis. The rutile and anatase both phases were present in XRD analysis of the synthesized materials. The particle size was found 24 and 82 nm in the case of La:Ni:TiO_2 nanocomposite and pure Titania respectively. The surface area of Titania and La:Ni:TiO_2 nanocomposite were found 6.4 and 43.2 m^2/g. The band gap energy of Titania and La:Ni:TiO_2 nanocomposite were found 3.2 eV and 3.0 eV respectively. The photodegradation of Citric Acid was investigated at different parameters such as temperature, concentration, pH of the reaction mixture, the dose of photocatalyst and time of illumination of visible light. The photodegradation of Citric Acid occurs 60-90% in presence of La:Ni:TiO_2 nanocomposite, while in presence of titania 10-18%. It is found that photodegradation of Citric Acid follows the first order kinetics.

Keywords: Titania, Nanocomposite, Photocatalyst, Photodegradation, Citric Acid

1. Introduction

Photocatalysed processes have grown in importance mainly due to their widespread applications in energy conversion, pollution abatement and the synthesis of new materials. Researchers are using photocatalysts for oxidative degradation of various non-biodegradable wastes. Fundamentally, photocatalysis deals with reactions which are initiated by electronically excited molecules generated by absorption of suitable radiation in the visible or near ultraviolet region [1, 2]. One of the most widely investigated and convenient class of photocatalysts is of metal oxide semiconductors. Thus, in practical terms, chemical reactions occurring in presence of semiconducting materials and light are known as photocatalytic reactions [3-4].

Most materials can be categorized as conductors, insulators, and semiconductors. Semiconductors are mainly of two types: (i) n-type and (ii) p- type. The n-type semiconductors are those, which exhibit conductivity due to the flow of majority electrons, while p- type semiconductors exhibit conductivity due to the presence of positively charged majority holes [5-7]. The energy gap (band gap) between valence band (highest occupied molecular orbital, HOMO) and conduction band (lowest unoccupied molecular orbital, LUMO) in a semiconductor is such that these materials behave as a conductor under certain conditions i.e., on exposure to light or at high temperature [8-10].

Titania (TiO_2) is the one of the mostly used as a semiconductor which has unique properties. It is inert and resistant to corrosion, and it requires little post-processing, making it inexpensive. Titania (TiO_2) powders possess interesting optical, dielectric, and catalytic properties, which leads to industrial applications such as pigments, fillers, catalyst supports, and photocatalysts [11-12]. It has been demonstrated that the final properties of this material depend on size, morphology and crystalline phase of the prepared TiO_2 nanopowder. The band gap energy of Titania is Eg = 3.2 eV. Therefore it is capable of absorbing only 5% UV light which is present in the solar spectrum [13]. Several investigations have been reported that the doping of metals and nonmetal decreases the band gap energy of Titania by the formation of sub-band [14].

In photocatalysis, light is absorbed by a semiconductor.

Today, semiconductors are usually selected as photocatalysts, because semiconductors have a narrow band gap between the valence and conduction bands. In order for photocatalysis to proceed, the semiconductors need to absorbed energy equal to or more than its energy gap. This movement of electrons forms e-/h+ or negatively charged electron/positively charged hole pairs [15-16]. The hole can oxidize donor molecules. In photogenerated catalysis, the photocatalytic activity (PCA) depends on the ability of the catalyst to create electron–hole pairs, which generate free radicals able to undergo secondary reactions. Its comprehension has been made possible ever since the discovery of water electrolysis by means of the titanium dioxide. Titanium dioxide used in photoelectrochemical splitting of water to hydrogen gas. It is also used as a self-cleaning agent [17-18].

Early reports show that Citric Acid may be moderately stable at close to UV-light [19], however, it will be decayed toward photolysis beneath 242 nm to items comparative should the individuals got under ionizing radiation [20–21]. In spite of thermally stable, iron (III) carboxylates would photochemically unstable: on account for Fe (III)–Cit, UV-What's more blue-light Push an effective photocatalysis with Fe (II) structuring Also oxidation of the ligand taken after toward decarboxylation [22-23]. Those accounted for last items are acetone, carbon dioxide, and acetone dicarboxylic Acid (3-oxoglutaric Acid, 3-OGA), on the same time the acetoacetic Acids were discovered concerning illustration intermediates [24]. AOTs investigations on Citric Acid would not enough. Something like that far, best two reports for oxidation through UV/TiO_2 photocatalysis Furthermore no additives need to give support to educated [25-27].

2. Methods and Materials

2.1. Synthesis of TiO_2 and La:Ni:TiO_2 Nanocomposite

In this study, La:Ni:TiO_2 nanocomposite were prepared by the solution impregnation method. TiO_2 powder (5g) was dispersed in 100 ml of the water: alcohol (10:1) solution with 10% or 0.5 g Nickel acetate and 5% or 0.25g Lanthanum nitrate. The dispersion is agitated continuously for 4 hours at 85°C temperature. After the heating and agitatison, the residue will be removed through filtration and was sintered for 4 hours in the presence of air at 500°C by keeping it in a silica crucible inside a muffle furnace. After sintering and slow annealing to room temperature, content was taken out from the furnace and was used as photocatalyst. Same procedure was used to synthesis the TiO_2 without Nickel acetate and Lanthanum Nitrate [28-29].

2.2. Photodegradation of Citric Acids

The samples of TiO_2 and La:Ni:TiO_2 nanocomposite were used as a photocatalyst in visible light for the photodegradation of Citric Acid. A 5g/L of the photocatalyst was dispersed in the Citric Acid solution and the reaction mixture was illuminated with visible light by using the Tungsten lamp of 450 W, 100V while kept under agitation. The residual concentrations of Citric Acid were measured by titrimetrically at different time intervals. In this study, investigated the photocatalytic behavior of TiO_2 and La:Ni:TiO_2 nanocomposite nanocomposites towards photo-degradation of Citric Acid [30-33].

3. Result

3.1. X-Ray Diffraction Analysis

The obtained X-Ray diffraction patterns of TiO_2 and La:Ni:TiO_2 nanocomposite are shown in Figure. 1. The observed pattern of peaks, when compared with the standard JCPDS database, suggested that, in prepared TiO_2 samples, major peaks at 2θ angles 25.5, 37.2, 48.3 and 55.4° correspond to anatase phase, whereas major peaks at 2θ angles 26.9, 28.2, 42.6 and 54.2° indicate the presence of rutile phase. In the case of La:Ni:TiO_2 nanocomposite sample, the observed XRD pattern indicates not only a decrease in the peak intensity, compared to TiO_2 but even the absence of some originally observed TiO_2 peaks. Some peaks are slightly shifted and their theta value increased. This is, probably, due to the change in the crystallinity, grain fragmentation, and partial amorphization, when the TiO_2 samples were doped by lanthanum and nickel [34-35].

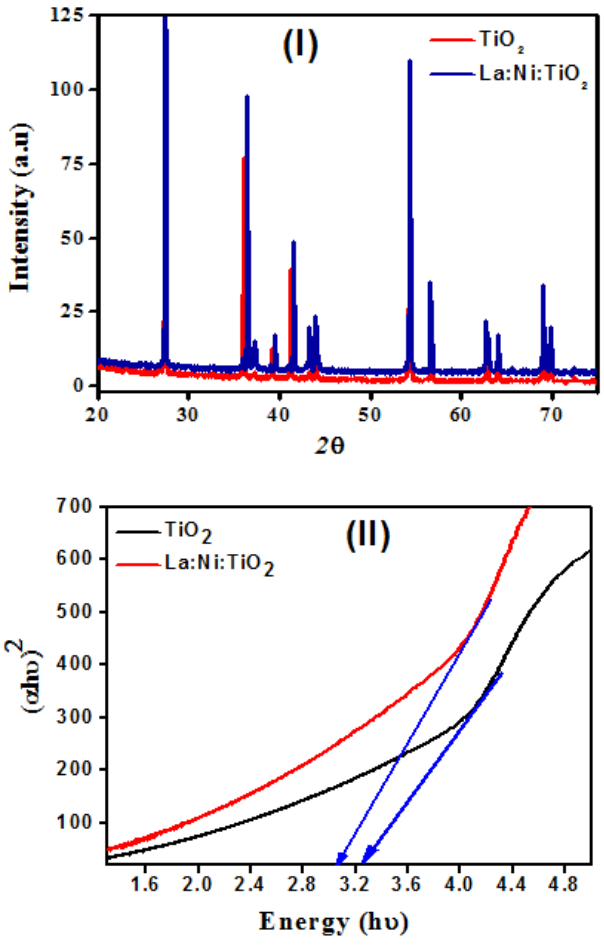

Figure 1. *(I) Observed XRD Pattern (II) Band Gap energy determination.*

3.2. Band Gap Energy Determination

The band gap of TiO_2 as calculated from the extrapolation of the absorption edge onto the energy axis is 3.2 eV and this is well reported. Figure 1 (II) shows the $(\alpha h\nu)^2$ versus $h\nu$ for a direct transition, where α is the absorption coefficient and $h\nu$ is the photon energy, $h\nu = (1239/\lambda)$ eV, where λ is the wavelength in nanometers. The value of $h\nu$ extrapolated to $\alpha = 0$ gives an absorption energy, which corresponds to a band gap Eg. The extrapolation of graph yields an Eg value of 3.2 eV which is, in fact, the band gap of Titania. But for the sample of La:Ni:TiO_2 nanocomposite the indirect plot yield band gap values of 3.0 eV [36-37]. The band gap energy is decreasing in La:Ni:TiO_2 nanocomposite because the lanthanum and Nickel forms a sub-band level between the valence band and the conduction band.

3.3. Determination of Average Size of Crystal in Samples

Scherrer's calculations were attempted to know the average size of crystal in the samples. Although, Scherrer's calculations are only approximate in nature, but definitely provide a first-hand idea of the average size of the crystal in the samples, which may be quite accurate, provided the size of crystal is below 100 nm. The results of Scherrer's calculations are presented in Table 1. The Scherrer's formula is given in equation 1 [35]. The results suggest an average size of the crystal in the samples lying in nm range.

$$B = \frac{0.9\lambda}{t\ Cos\theta} \quad (1)$$

Table 1. *Average size of crystal in the samples by Scherrer's calculation.*

Sample	Crystal size (nm)
TiO_2	82
La:Ni:TiO_2 nanocomposite	24

3.4. Scanning Electron Microscopy (SEM) and Transmission Electron Microscopy (TEM)

The morphology of the samples was investigated by scanning electron microscopy and it resumes the most interesting outcomes. Figure 2a and 2b clearly show that both the prepared samples are obtained agglomerate in nanometric dimension. The doping of Lanthanum and Nickel are indicating that the particle size reduces due the penetration of Lanthanum and Nickel in the lattice of titanium dioxide [38].

TEM analysis of materials was used to examine the crystallite size, morphology. The prepared TiO_2 powders consist of both spherical and semi-spherical shape; on the contrary, the particle of La:Ni:TiO_2 nanocomposite has mostly spherical morphology. It can be estimated that the particle size of TiO_2 and La:Ni:TiO_2 nanocomposite nanocomposites in Figure (2c) and (2d) are nanoscale with the grain size less than 100 nm [39].

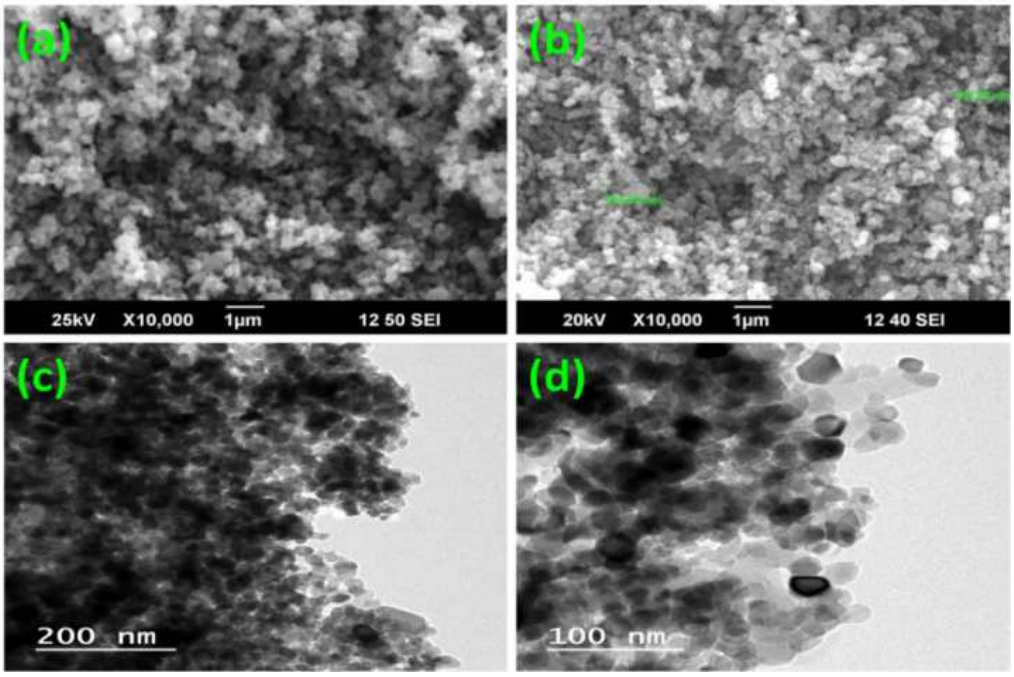

Figure 2. *Observed SEM and TEM image of (a and c) TiO_2 (b and d) La:Ni:TiO_2 nanocomposite.*

3.5. FT-IR Spectroscopy

FT-IR spectra of undoped and 5.0% La and 10.0% Ni impregnated TiO_2 samples (Figure 3) showed the peaks corresponding to stretching vibrations of the O-H and bending vibrations of the adsorbed water molecules around 3350-3450 cm^{-1} and 1620-1635 cm^{-1}, respectively. The broad intense band below 820, 804, 592 and 456 cm^{-1} is due to Ti-O-Ti vibrations, the shift to the higher wave numbers and sharpening of the Ti-O-Ti band in Figure 3 is due to the decrease in crystal size of the photocatalyst. In addition, the surface hydroxyl groups in TiO_2 increase with the increase of La and Ni loading, which is confirmed by increase in

intensity of the corresponding peaks. The FTIR spectra shows strong band at 1075 cm^{-1} corresponds to the vibration of Ni–O bond and it is confirm the penetration of Lanthanum and Nickel in Titania [40].

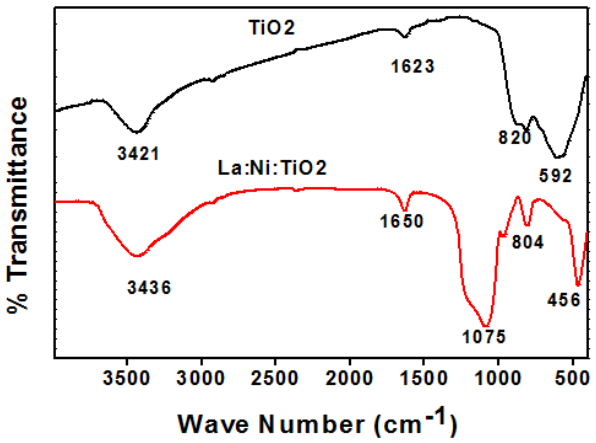

Figure 3. *FT-IR Spectra of (a) TiO_2 (b) La:Ni:TiO_2.*

3.6. UV-Vis Diffuse Reflectance Spectroscopy (DRS)

Aqueous suspensions of the samples were used for the UV absorption studies. The blue shift that is observed in the absorption spectra with the decrease in particle size has been reported earlier. The absorption spectrum of TiO_2 consists of a single broad intense absorption around 378 nm due to the charge transfer from the valence band to the conduction band [41]. Figure 4 shows the absorbance of prepared samples. The undoped TiO_2 showed absorbance in the shorter wavelength region while La:Ni:TiO_2 nanocomposite results showed a red shift in the absorption onset value in the case of La and Ni impregnated Titania. The impregnation of La and Ni ions into TiO_2 could shift its optical absorption edge from UV into visible light range, due to prominent change in TiO_2 band gap was observed [42].

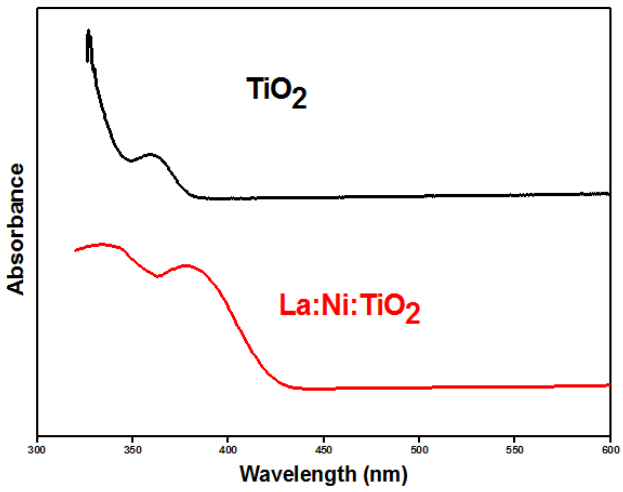

Figure 4. *UV- Vis. Spectra of TiO_2 and La:Ni:TiO_2.*

3.7. Surface Area Analysis (B. E. T)

The specific surface area, pore volume and average pore size of the TiO_2 and La:Ni:TiO_2 nanocomposite as-prepared photocatalyst were characterized by using the N_2 adsorption technique (showing in Figure 5) *BET (*belsorp Japan*)*. Table - 2 summarizes their physical properties. The TiO_2 modified by Lanthanum and Nickel are fragmentized to some extent during thermal treatment, leading to a marked increase of the surface areas and the average pore radius size and decreasing of the pore volume [43-44].

Table 2. *Phase ssurface areas, pore volume, pore radius of TiO_2 and La:Ni:TiO_2 nanocomposite.*

Sample	Surface area (m^2/g)	Pore volume (cm^3/g)	Pore radius (nm)
TiO_2	6.4	0.018	11
La:Ni:TiO_2 nanocomposite	43.2	0.031	6

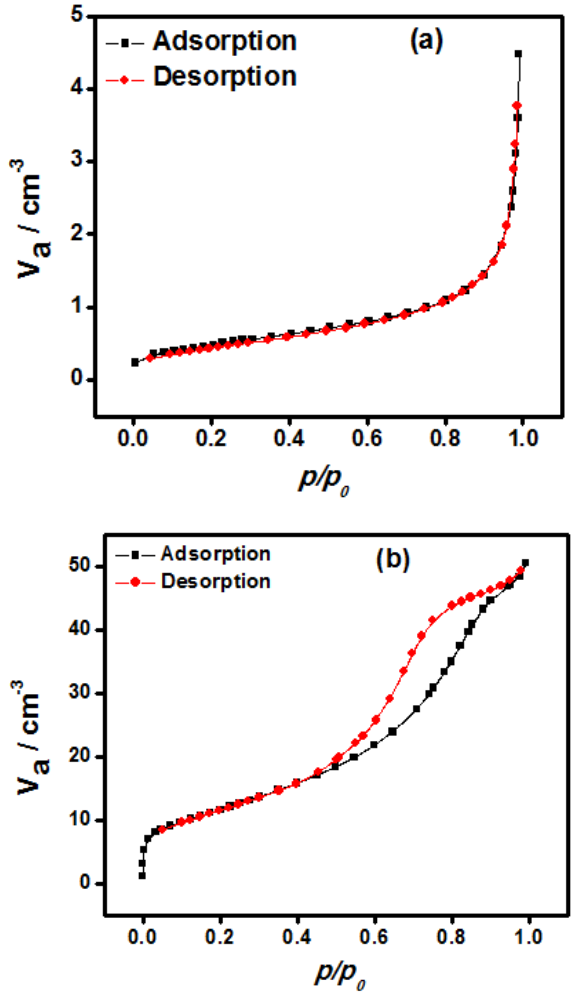

Figure 5. *Adsorption desorption plot of the (a) TiO_2 (b) La:Ni:TiO_2 nanocomposite.*

3.8. Photo-Degradation of Citric Acid

In this study, photocatalytic degradation of Citric Acid was investigated. The measured values of residual concentration of Acid in the reaction mixture at different times of illumination (or reaction time) have been shown in Figures 6 (I, II, III and IV) [45-53].

3.8.1. Effect of Temperature

In the present research, it is found that the temperature has a great effect on the photodegradation of Citric Acid. The photocatalytic efficiency can be increased about 2-3 times if the temperature increased from 30°C to 40°C because the solar energy includes visible light, which can be used to activate the photocatalytic course, which increases the temperature of the photocatalytic system. The experiments showed that Citric Acid cannot be photodegraded if TiO_2 or Visible light was not used, indicating that Citric Acid cannot be pyrolyzed by heating with the heating temperature which was less than 40°C and self-degraded by absorbing irradiation. Only when both the photocatalyst and visible light were used, the Citric Acid was efficiently degraded, shown in Figure 6 (I). The photodegradation of Citric Acid was 47% at 30°C in presence of La:Ni:TiO_2 nanocomposite when the temperature of the reaction raise 10°C, the photodegradation was found 72%, whereas in presence of TiO_2 there is no significant effect of temperature was observed. The photodegradation of Citric acid was found 2-10% in presence of Neat Titania. Hence, La:Ni:TiO_2 nanocomposite can serve as an effective photocatalyst than TiO_2 [45, 46].

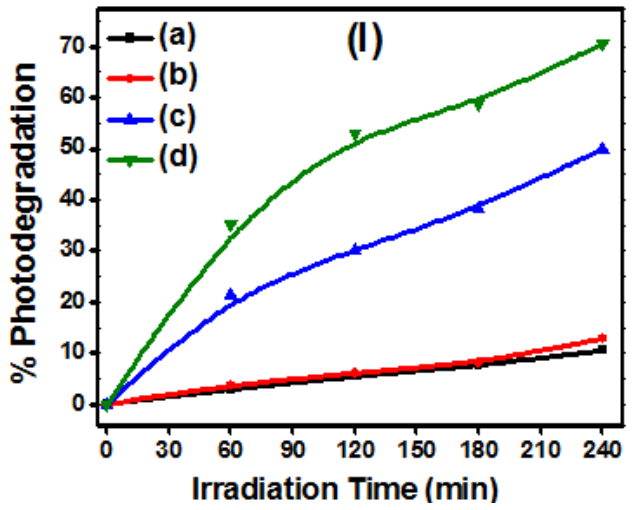

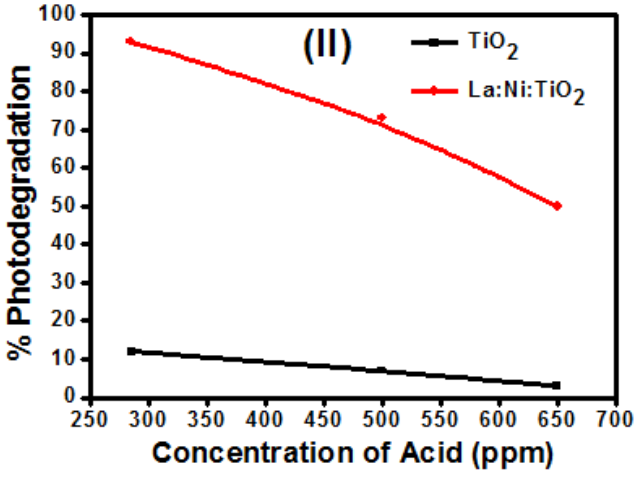

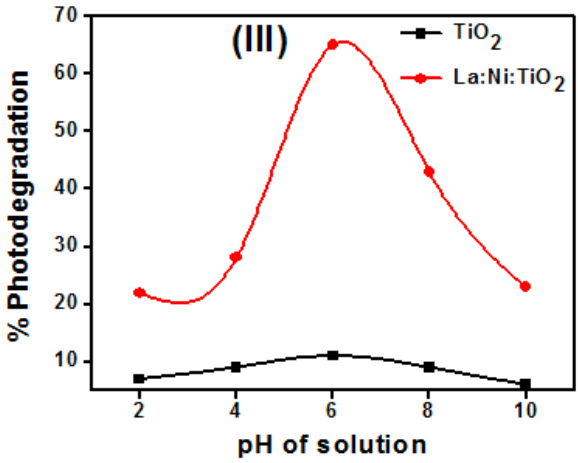

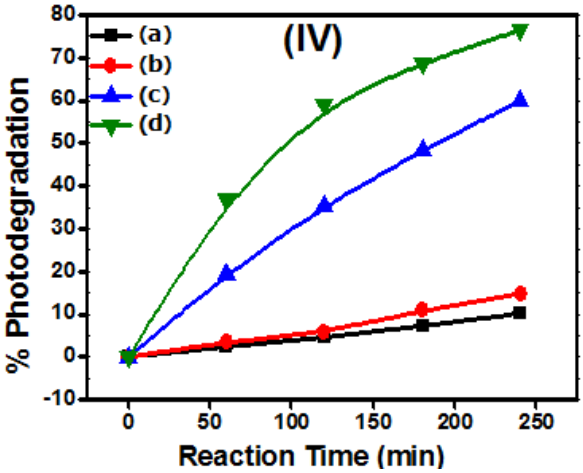

Figure 6. *(I) Effect of temperature on Photodegradation of Citric Acid (a) TiO_2 at 30°C (b) TiO_2 at 40°C (c) La:Ni:TiO_2 nanocomposite at 30°C (d) La:Ni:TiO_2 nanocomposite at 40°C.(II) Effect of Concentration (III) Effect of pH (IV) Effect of amount (a) TiO_2 with 5g/L (b) TiO_2 10g/L (c) La:Ni:TiO_2 nanocomposite with 5g/L (d) La:Ni:TiO_2 nanocomposite with 10g/L.*

3.8.2. Effect of Concentration of Citric Acid

Effect of Citric Acid concentration keeping the catalyst loading constantly at 1000 mg/liter in the Acid solution, the effect of varying concentration of the Acid was studied on its rate of its degradation (from 285 ppm to 650 ppm) as given in Figure. 6 (II). With increasing concentration of Citric Acid the rate of degradation was found to decrease. This is because as the number of Acid molecules increase, therefore, the amount of light (quantum of photons) penetrating the Acid solution to reach the catalyst surface is reduced owing to the hindrance in the path of light. Thereby the formation of the reactive hydroxyl and superoxide radicals is also simultaneously reduced. Thus there should be an optimum value maintained for the catalyst and the Citric Acid concentration, wherein maximum efficiency of degradation can be achieved [46, 48, 52].

3.8.3. Effect of PH

The photodegradation reaction was also carried out under varying pH conditions from (2 to 10), by adjusting with NaOH, with TiO_2 kept at constant amounts of 200 mg in 20 ml of citric acid solutions. The reaction was found to have

high rates at neutral ranges of pH. While at low pH, 10-20% photodegradation of citric acid was observed in presence of pure TiO_2 whereas 68% in presence of La:Ni:TiO_2 nanocomposite. The maximum photodegradation was observed at 6 pH, but after 6 pH the photodegradation is rapidly decreasing and showing in Figure 6 (III). This implies that acidic conditions are favourable towards the formation of the reactive intermediates that is hydroxyl radicals is significantly enhanced, which further help in enhancing the reaction rate. On the other hand, in highly acidic highly basic medium conditions is relatively less favourable for the formation of reactive intermediates and hence less spontaneous [47-48, 51].

3.8.4. Effect of Photocatalyst and Their Amount

It is clear from the results shown in Figure. 8 that both TiO_2 and La:Ni:TiO_2 nanocomposite are proving as an effective photocatalyst for the degradation of Citric Acids. However La:Ni:TiO_2 nanocomposite seems to be more effective as a photocatalyst for the degradation of Citric Acids. The prominent degradation of Citric Acids was found in 3-hour study in the presence of La:Ni:TiO_2 nanocomposite in comparison to the pure TiO_2. It is showing in Figure 6 (IV). This is because of the surface area of La:Ni:TiO_2 nanocomposite is greater than TiO_2. Hence La:Ni:TiO_2 nanocomposite is absorbing the more photon on its surface than TiO_2 [49, 50, 53]. Hence the adsorption of the Citric Acid molecule on the surface of photocatalyst increased and photodegradation of Acid become increase. The effect of photocatalyst amount has been investigated for the degradation of citric acid. The amount of photocatalyst increases the photodegradation of Citric Acid increase in both photocatalyst. The La:Ni:TiO_2 nanocomposite is the superior photocatalyst than the pure TiO_2. Because the number of the active site in La:Ni:TiO_2 nanocomposite is greater than TiO_2 [53]. It is observed that La:Ni:TiO_2 nanocomposite is the more effective photocatalyst than TiO_2.

3.9. Mechanism of Photocatalysis

The acceleration of a chemical transformation by light in the presence of a catalyst is called photocatalysis. The catalyst may accelerate the photoreaction by interaction with the substrate in its ground or excited state and/or with a primary photoproduct, depending upon the mechanism of the photoreaction remaining unaltered at the end of each catalytic cycle. Heterogeneous photocatalysis is a process in which two active phases, solid and liquid are present. The solid phase is a catalyst, usually a semiconductor [54]. The molecular orbital of semiconductors has a band structure. The bands of interest in photocatalysis are the populated VB and it is largely vacant CB, which is commonly characterized by band gap energy (*E*bg). The semiconductors may be photoexcited to form electron-donor sites (reducing sites) and electron-acceptor sites (oxidising sites), providing great scope for redox reaction [55]. When the semiconductor is illuminated with light ($h\nu$) of greater energy than that of the band gap, an electron is promoted from the VB to the CB leaving a positive hole (h^+) in the VB and an electron (e^-) in the CB as illustrated in Figure. 7. If charge separation is maintained, the electron and hole may migrate to the catalyst surface where they participate in redox reactions with sorbed species. The VB and CB energies of the TiO_2 are estimated to be +3.1 and –0.1 V, respectively, which means that its band gap energy is 3.2 eV, and therefore, absorbs in the near UV light (l < 387 nm). Many organic compounds have a potential above that of the TiO_2 VB, and therefore, can be oxidized. In contrast, fewer organic compounds can be reduced since a smaller number of them have a potential below that of the TiO_2 CB. VB may react with surface-bound H_2O or OH– to produce the hydroxyl radical and e– cb is picked up by oxygen to generate superoxide radical anion (O_2 –), as indicated in the following Eqs. (2) – (6). Absorption of efficient photons by titania ($h\nu \geq Ebg = 3.2$ eV):

$$TiO_2 + h\nu \rightarrow TiO_2 + h^+_{VB} + e^-_{CB} \quad (2)$$

Formation of superoxide radical anion:

$$O_2 + e^- \rightarrow O_2^- \quad (3)$$

Neutralization of OH– group into OH by the hole:

$$(H_2O \Leftrightarrow H^+ + OH^-)_{ads} + h^+_{vb} \rightarrow {}^{\bullet}OH + H^+ \quad (4)$$

It has been suggested that the hydroxyl radical ($^{\bullet}OH$) and superoxide radical anions (O_2^-) are the primary oxidizing species in the photocatalytic oxidation processes. These oxidative reactions would result in the degradation of the pollutants as shown in the following Eqs. (5) and (6). Oxidation of the organic pollutants via successive attack by OH radicals:

$$R + {}^{\bullet}OH \rightarrow R + H_2O \quad (5)$$

or by direct reaction with holes

$$R + h^+ \rightarrow R.^+ \rightarrow \text{degradation products} \quad (6)$$

For oxidation reactions to occur, the VB must have a higher oxidation potential than the material under consideration. The redox potential of the VB and the CB for different semiconductors varies between +4.0 and –1.5 V vs. normal.

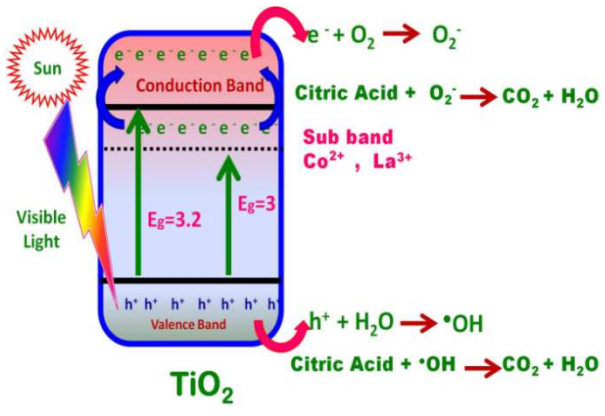

Figure 7. *Photocatalytic mechanism of degradation of citric acid.*

3.10. Kinetic Study

The pseudo-first-order rate constant (k, min^{-1}) for the photodegradation reaction of Citric Acid was determined through the following relation where k can be calculated from the plot of ln (C_o/C_t) against time (t), C_0 and C_t denote the initial concentration and reaction concentration, respectively.

$$\ln C_o/C_t = k_1 t \quad (7)$$

In addition, the linear feature of plots of ln (C_o/C_t) versus time (Figure 8) indicates that these photocatalytic degradation reactions follow the pseudo-first-order rate law [56-57].

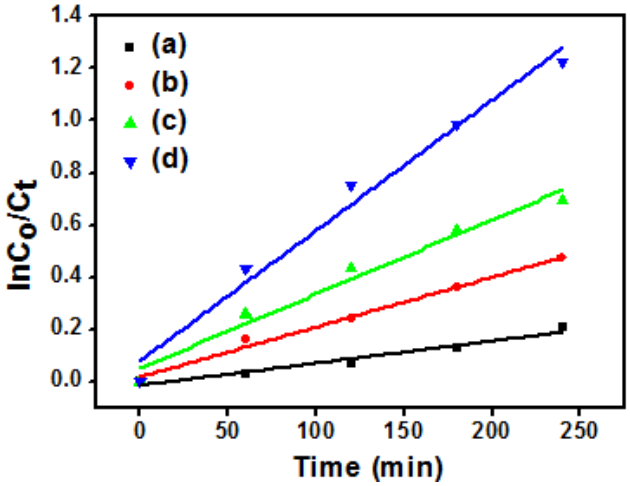

Figure 8. *Concentration vs time graphs for the determination of rate constant k for (a) TiO_2 with 30°C (b) TiO_2 with 40°C (c) La:Ni:TiO_2 nanocomposite with 30°C (d) La:Ni:TiO_2 nanocomposite with 40°C.*

The rate constant depends on temperature. If we increase 10°C temperatures then the rate constant becomes double or triple. Table 3 showing the effect of temperature on rate constant for synthesized TiO_2 and La:Ni:TiO_2 nanocomposite but in the case of La:Ni:TiO_2 nanocomposite the rate constant is greater than Titania [58].

Table 3. *Effect of temperature on rate constant.*

Photocatalyst	Temperature	Rate constant (min^{-1})
TiO_2	30°C	1.29×10^{-3}
TiO_2	40°C	3.8×10^{-3}
La:Ni:TiO_2	30°C	2.54×10^{-3}
La:Ni:TiO_2	40°C	4.83×10^{-3}

4. Conclusions and Discussions

In the present study, we prepared the nanocomposites of Titania by a chemical method and photocatalytic degradation of Citric Acid in the presence of nanocomposites of Titania and La:Ni:TiO_2 nanocomposite was done. The prepared material was subjected to XRD analysis which gives the rutile and anatase both phases were present in the prepared sample. SEM analysis also proves that material was in nano dimension. Applying the Scherrer's calculations through which particle size was found 24 and 82 nm in the case of La:Ni:TiO_2 nanocomposite and pure Titania respectively. The prepared sample of Titania and La:Ni:TiO_2 nanocomposite were subjected to photocatalytic degradation of Citric Acid was done. The prominent degradation was found in the case of La:Ni:TiO_2 nanocomposite nanocomposites. The photodegradation of Citric Acid investigated at various parameters, such as pH, Concentration, temperature, photocatalyst nature and the amount of photocatalyst. The photodegradation of Citric Acid occurs 60-90% in presence of La:Ni:TiO_2 nanocomposite, while in presence of titania 10-18%. The photocatalytic degradation of Citric Acid follows the pseudo-first-order rate law.

Acknowledgements

We thanks for financial assistance to UGC, Government of India is acknowledged. The authors acknowledge the support provided by the Babasaheb Bhimrao Ambedkar University, Lucknow.

References

[1] Jacoby W. A., Maness P. C., Wolfrum E. J., Blake D. M., Fennell J. A., Environ. *Sci., Tech.,* 32 (1998) 2650.

[2] Hoffmann M. R., Martin S. T., Choi W. Y., Bahnemann D. W., *Chem. Rev*., 95 (1995) 69.

[3] Fujishima A., Hashimoto K., Watanabe T., *BKC*, Tokyo, 1999.

[4] Ziolli R. L., Jardim W. F., J. Photochem. Photobiol. A Chem. 147 (2002) 205.

[5] Berger T., Sterrer M., Diwald O., Knozinger E., Panayotov D., Thompson T. L., Yates J. T., *J., Phys., Chem.,* B 109 (2005) 6061.

[6] Szczepankiewicz S. H., Moss J. A., Hoffmann M. R., *J., Phys., Chem.,* B 106 (2002) 2922.

[7] Arabatzis I. M., Stergiopoulos T., Bernard M. C., Labou D., Neophytides S. G., Falaras P., Appl. *Catal. B Environ*. 42 (2003) 187.

[8] Arabatzis I. M., Stergiopoulos T., Andreeva D., Kitova S., Neophytides S. G., Falaras P., *J., Catal.* 220 (2003) 127.

[9] Hu C., Tang Y. H., Jiang Z., Hao Z. P., Tang H. X., Wong P. K., Appl. Catal. A Gen. 253 (2003) 389.

[10] Keleher J., Bashant J., Heldt N., Johnson L., Li Y. Z., *World J., Microbiol. Biotechnol*. 18 (2002) 133.

[11] Wang C., Wang T. M., Zheng S. K., Physica E 14 (2002) 242.

[12] Sun B., Vorontsov A. V., Smirniotis P. G., Langmuir 19 (2003) 3151.

[13] Li F. B., Li X. Z., Chemosphere 48 (2002) 1103.

[14] Vamathevan V., Amal R., Beydoun D., Low G., McEvoy S., J. Photochem. Photobiol. A Chem. 148 (2002) 233.

[15] Paunesku T., Rajh T., Wiederrecht G., Maser J., Vogt S., Stojicevic N., Protic M., Lai B., J. Oryhon, M. Thurnauer, G. Woloschak, Nat. Mater. 2 (2003) 343.

[16] Rajh R., Nedeljkovic J. M., Chen L. X., Poluektov O., Thurnauer M. C., *J., Phys., Chem*. B 103 (1999) 3515.

[17] Brune A., Jeong G., Liddell P. A., Sotomura T., Moore T. A., Moore A. L., Gust D., Langmuir 20 (2004) 8366.

[18] Krishna V., Pumprueg S., Lee S. H., Zhao J., Sigmund W., Koopman B., Moudgil B. M., *Process Saf., Environ. Prot*. 83 (2005) 393.

[19] Lee S. H., Pumprueg S., Moudgil B., Sigmund W., Colloids Surf. B Biointerfaces 40 (2005) 93.

[20] Krishna V., Noguchi N., Koopman B., Moudgil B., *J. of Colloid and Interface Science* 304 (2006) 166.

[21] Zhang L., kanki T., Sano N., Toyoda A., *J. Solar Energy* 70 (4) (2001) 331.

[22] Song K. H., Park M. K., Kwon V. T., Le K. W., Chang W. J., Lee W. I., Chem. mater, 13, (2001)2349.

[23] Ameta S. C., Punjabi P. B., Rao P., and Singhle B., *J. Indian Chem Soc.,* 77, (2000)157.

[24] Ohtani B., Ogawa Y., and Nishimoto S., *J. Phys. Chem*. B, 101, (1997) 3746.

[25] Cao F., Oskam G. J., Meyer S., and Searson P. C., *J*. Phy. Chem. B, 100, (1996)17021.

[26] Armelao L., Barreca D., Bertapelle M., Balttaro G., Sada C., and Tondello E., thin solid films, 442, (2003), 48.

[27] Balamurugan B., Mehta B. R., Thin solid films, 396, (2001), 90.

[28] Beydoun D., and Amal R., *J. Phys. Chem. B,* 104 (2000) 4387.

[29] A. Kumar, G. Hitkari, M. Gautam, S. Singh, G. Pandey, *Int. Adv. Res. J. in Science, Eng. And Tech.*, *2 (2015) 50-55,* DOI 10.17148/IARJSET.2015.21208.

[30] Mills A., Jishun W., *J.* of Photochemistry and Photobiology A: Chem. 118 (1998) 53.

[31] Draper R. B., and Anne F. M., *Langmuir*, 6, (1990)1396.

[32] Jaeger C. D., Bard A. J., *J., Am., Chem., Soc.* 102. (1980)5435.

[33] Bickley R. I., Munuera G., and Stone F. S., *J*. Catal, 31, (1973) 398.

[34] Shiraishi F., and Kawanishi C., *J. Phys. Chem*., A 108, (2004)10491.

[35] Cullity B. D., Stock S. R., (2001), Elements of X-Ray Diffraction, Third Edition, and New Jersey: Prentice-Hall, Inc.

[36] A. Kumar, G. Pandey, Chem Sci J 8 (2017) 164. doi: 10.4172/2150-3494.1000164.

[37] Richard C., Bosquet F., Pilichowski J., *J.* of Photochemistry and Photobiology A: Chem. 108 (1997) 45.

[38] Rupa A. V., Divakar D., Sivakumar T., Catal Lett, 132: (2009), 259.

[39] Mahshid S., Askari M., Sasani Ghamsari M., Journal of Materials Processing Technology 189 (2007) 296.

[40] A. Kumar, D. Kumar, G. Pandey. J. Technological Advances and Scientific Res.; 2(4) (2016) 166-169, DOI: 10.14260/jtasr/2016/29.

[41] Kralova M., Levchuk I., Kasparek V., Sillanpaa M., Cihlar J., *Chinese Journal of Catalysis, 36 (2015) 1679.*

[42] Albetran H., O'Connor B. H., Low I. M., *Materials & Design, 92 (2016) 480.*

[43] Nair R. R., Arulraj K. R., Devi S., *Materials Today: Proceedings, 3 (2016) 1643.*

[44] Koh P. W., Hayrie M., Hatta M., Ong S. T., Yuliati L., Lee S. L., *Journal of Photochemistry and Photobiology A: Chemistry, 332 (2017) 215.*

[45] Khan A. W., Ahmad S., Hassan M. M., Naqvi A. H., *Optical Materials, 38 (2014) 278.*

[46] A. Kumar, G. Hitkari, M. Gautam, S. Singh, G. Pandey, Int. J. of Inno. Res. in Science, Eng. and Techn. 4 (2015) 12721-12731, DOI: 10.15680/IJIRSET.2015.0412097.

[47] Tang W., Qiu K., Zhang P., Yuan X., *App. Surface Science, 362 (2016) 545.*

[48] A. Kumar and G. Pandey, Chemical Science Transactions 2017, 6(3), 385-392, DOI: 10.7598/cst2017.1378.

[49] Chen D., Ray A. K., Appl. Catal. B: Environ. 23 (1999) 143.

[50] A. Kumar, G. Pandey. American Journal of Nano Research and Applications. 5, (2017) 40-48, doi: 10.11648/j.nano.20170504.11.

[51] Yang J., Chen C., Ji H., Wanhong M., and Zhao J., J. Phys. Chem. B, *109* (2005) 21900.

[52] A. Kumar, G. Pandey, *Desalination and Water Treatment,* 71 (2017) 406–419, doi: 10.5004/dwt.2017.20541.

[53] Vulliet E., Chovelon J. M., Guillard C., Herrmann J. M., J. Photochem. Photobiol. A: Chem. 159 (2003) 71.

[54] Matthews R. W., J. Applied Catalysis. 111 (1988) 264.

[55] Vautier M., Guillard C., Herrmann J. M., J. Catal. 201 (2001) 46.

[56] Freundlich H., Ueber D., J. Phys. Chem. 57 (1907) 385.

[57] Langmuir I., J. Am. Chem. Soc. 40 (1918) 1361.

[58] Ono Y., Rachi T., Okuda T., Yokouchi M., Kamimot Y., Nakajima A., Okada K., J. of Physics and Chemistry of Solids 73 (2012) 343.